Article

Characterizing Adsorption Performance of Granular Activated Carbon with Permittivity

Yang Yang, Chao Shi, Yi Zhang, Jinghua Ye, Huacheng Zhu * and Kama Huang

College of Electronic and Information Engineering, Sichuan University, Chengdu 610065, China;
yyang@scu.edu.cn (Y.Y.); shichaoscu@126.com (C.S.); yizhangscu@126.com (Y.Z.);
2015322050010@stu.scu.edu.cn (J.Y.); kmhuang126@126.com (K.H.)
* Correspondence: hczhu@scu.edu.cn; Tel.: +86-135-5009-1988

Abstract: A number of studies have achieved the consensus that microwave thermal technology can regenerate the granular activated carbon (GAC) more efficiently and energy-conservatively than other technologies. In particular, in the microwave heating industry, permittivity is a crucial parameter. This paper developed two equivalent models to establish the relationship between effective complex permittivity and pore volume of the GAC. It is generally based on Maxwell-Garnett approximation (MGA) theory. With two different assumptions in the model, two quantificational expressions were derived, respectively. Permittivity measurements and Brunauer–Emmett–Teller (BET) testing had been introduced in the experiments. Results confirmed the two expressions, which were extremely similar. Theoretical and experimental graphs were matched. This paper set up a bridge which links effective complex permittivity and pore volume of the GAC. Furthermore, it provides a potential and convenient method for the rapid assisted characterization of the GAC in its adsorption performance.

1. Introduction

Granular activated carbon (GAC) has a remarkable adsorption capacity due to its extensively developed internal pore structure and large specific surface area [1], making it an ideal medium for adsorbing impurities and purifying both aqueous solutions [2–4] and flue gas [5]. To recycle and conserve the limited resources, the GAC needs to be regenerated. Microwave thermal treatment for regenerating GAC is promising [6–8]. For instance, Ania et al. [9] studied the effect of different heating mechanisms (a conventional electric furnace versus microwave device) to regenerate the activated carbon exhausted with phenol. Regeneration time was considerably shortened in the microwave device compared to regeneration with the conventional electric furnace. Meanwhile, the porous structure of the regenerated AC using the microwave device was more efficient than that using the conventional electric furnace.

However, the conventional characterization method to evaluate the adsorption performance of the generated GAC is time-consuming. It usually takes dozens of hours to accomplish the test [10]. This paper established the relationship between effective permittivity and pore volume of the GAC. Many studies indicate that either pore volume [11] or pore structure [12], especially pore size distribution (PSD) [13,14] is the most important adsorbent property for GAC. With the development of the microwave measurement method in complex permittivity, e.g., resonant cavity method [15–17], perturbation method [15,18,19], transmission and reflection method [20–22], it is convenient to get the complex permittivity data of the GAC.

This paper proposes two equivalent models to establish the relationship between effective complex permittivity (ε_{eff}) and pore volume (v_g) for a given commercial GAC. Brunauer–Emmett–Teller (BET) testing and microwave permittivity measurement with perturbation method are introduced below to verify the relationship between effective complex permittivity and pore volume.

2. Derivation

The Maxwell-Garnett (MG) effective medium theory [23], originally derived by neglecting the density fluctuations of dipolar character of scatterers, is the most widely used theory to characterize the complex permittivity of medium [24]. Li et al. [25] applied it in characterizing complex permittivity of solids. It can predict the effective permittivity of a mixture based on the equation:

$$\left(\frac{\varepsilon_m - \varepsilon_h}{\varepsilon_m + 2\varepsilon_h} \right) = \delta_i \left(\frac{\varepsilon_i - \varepsilon_h}{\varepsilon_i + 2\varepsilon_h} \right) \tag{1}$$

where ε_m, ε_h and ε_i are the complex permittivity of the mixture, host medium and inclusions, respectively, and δ_i is the volume fraction of the inclusions. Equation (1) is valid under the condition of low volume fractions. It is necessary to make sure that δ_i does not exceed 0.5.

In this particular case, we simply regard the pure GAC with no pore structure, namely the "the ideal pure GAC", as the host medium. Its complex permittivity is characterized as ε_{GAC}^t. The value of ε_{GAC}^t should only exist in theory as it can not be measured directly. Similarly, we regard the pore as the inclusions. Thus, the whole GAC is composed of pure GAC and pores. The complex permittivity (ε_{eff}) of the GAC should be the mixture.

With several steps of elementary algebraic transformation, the MG effective permittivity represented by Equation (1) can be solved by:

$$\varepsilon_{eff} = \varepsilon_{GAC}^t \frac{2\delta_i\left(\varepsilon_i - \varepsilon_{GAC}^t\right) + \varepsilon_i + 2\varepsilon_{GAC}^t}{2\varepsilon_{GAC}^t + \varepsilon_i + \delta_i\left(\varepsilon_{GAC}^t - \varepsilon_i\right)} \tag{2}$$

We simply assume the pore is full of air, which means $\varepsilon_i = 1$. Taking the defining equation of δ_i into account, we obtain:

$$\begin{cases} \varepsilon_{eff} = \varepsilon_{GAC}^t \frac{1 + 2\delta_i + 2(1-\delta_i)\varepsilon_{GAC}^t}{1 - \delta_i + (2+\delta_i)\varepsilon_{GAC}^t} \\ \delta_i = \frac{V_i}{V_{total}}, (0 < \delta_i < 0.5) \end{cases} \tag{3}$$

where V_i is the volume of the inclusions and V_{total} is the total volume of the whole GAC. Particularly, when it is for the unit mass of the GAC, V_i turns to be a significant physical concept–the pore volume (v_g) in cm^3/g.

We introduce the granule density (ρ_g), which is defined as the mass (m_0) divided by the volume (v_0) in a single granule, i.e., $\rho_g = m_0/v_0$. This approach offers two ways to build our model to make the connection between ε_{eff} and v_g.

2.1. Model A

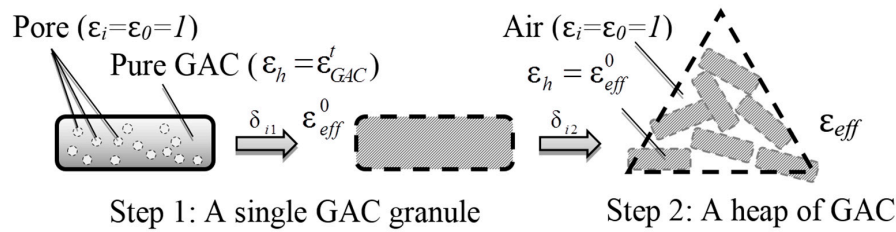Step by step with applying the MGA Equation (3) twice. As is shown below (Figure 1), it takes two steps to make the connection between ε_{eff} and v_g.

Figure 1. Schematic diagram for deriving the relationship between ε_{eff} and v_g.

Step 1: Focusing on a single GAC granule.

Volume fraction δ_i of a single granule should be expressed as follows:

$$\delta_i = \frac{V_i}{V_{total}} = \frac{v_g m_0}{v_0} = v_g \rho_g \tag{4}$$

Substituting this relationship into Equation (3):

$$\varepsilon_{eff}^0 = \varepsilon_{GAC}^t \frac{1 + 2v_g\rho_g + 2\varepsilon_{GAC}^t - 2v_g\rho_g\varepsilon_{GAC}^t}{1 - v_g\rho_g + 2\varepsilon_{GAC}^t + v_g\rho_g\varepsilon_{GAC}^t} \tag{5}$$

Step 2: Considering a heap of GAC.

Whereby the volume fraction is calculated as follows:

$$\delta_i = \frac{V_i}{V_{total}} = \frac{V_{heap} - V_{host}}{V_{heap}} = \frac{V - M/\rho_g}{V} = 1 - \frac{M}{V\rho_g} \tag{6}$$

where M and V are the mass and the volume of the heap, respectively, and V_{host} is the volume of the host media (i.e., the total volume of the GAC granule in the heap).

Similarly, substituting Equation (6) into (3):

$$\varepsilon_{eff} = \varepsilon_{eff}^0 \frac{3 - \frac{2M}{V\rho_g} + \frac{2M}{V\rho_g}\varepsilon_{eff}^0}{\frac{M}{V\rho_g} + 3\varepsilon_{eff}^0 - \frac{M}{V\rho_g}\varepsilon_{eff}^0} \tag{7}$$

Equation (7) is simplified by multiplying the numerator and denominator with $V \cdot \rho_g$:

$$\varepsilon_{eff} = \varepsilon_{eff}^0 \frac{3V\rho_g - 2M + 2M\varepsilon_{eff}^0}{M + 3V\rho_g\varepsilon_{eff}^0 - M\varepsilon_{eff}^0} \tag{8}$$

where M, V, ρ_g, and ε_{GAC}^t are constant. M, V, and ρ_g can be measured directly and conveniently. The independent variable v_g is implied in the expression of ε_{eff}^0 in Equation (5).

2.2. Model B

Directly focus on a heap of GAC, applying MGA Equation (3) only once. In this particularly situation, we simply treat porosity both in the GAC granule (i.e., total pore volume) and between each GAC granules the same. They are all regarded as inclusions, sharing the same permittivity: $\varepsilon_i = \varepsilon_0 = 1$. In this instance, the volume fraction will be less complicated, which is expressed as follows:

$$\delta_i = \frac{V_i}{V_{total}} = \frac{V_{pores} + V_{air}}{V_{heap}} = \frac{Mv_g + \left(V - M/\rho_g\right)}{V} = 1 + \left(v_g - \frac{1}{\rho_g}\right)\frac{M}{V} \tag{9}$$

Substituting Equations (9) into (3), yielding:

$$\varepsilon_{eff} = \varepsilon_{GAC}^t \frac{3 + \frac{2M}{V}\left(v_g - 1/\rho_g\right) - \frac{2M}{V}\left(v_g - 1/\rho_g\right)\varepsilon_{GAC}^t}{-\frac{M}{V}\left(v_g - 1/\rho_g\right) + \left[3 + \frac{M}{V}\left(v_g - 1/\rho_g\right)\right]\varepsilon_{GAC}^t} \tag{10}$$

Multiply the numerator and denominator with $V \cdot \rho_g$, and simplify it, finally we obtain:

$$\varepsilon_{eff} = \varepsilon_{GAC}^t \frac{3V\rho_g + 2M\left(v_g\rho_g - 1\right) - 2M\left(v_g\rho_g - 1\right)\varepsilon_{GAC}^t}{3V\rho_g\varepsilon_{GAC}^t - M\left(v_g\rho_g - 1\right) + M\left(v_g\rho_g - 1\right)\varepsilon_{GAC}^t} \tag{11}$$

Similarly, M, V, ρ_g, and ε_{GAC}^t are constant or measurable, it is obvious that the Equation (11) achieved the goal to make the connection between ε_{eff} and v_g.

3. Experiment Setup

3.1. Materials and Sample Preparations

The original GAC came from the commercial activated carbon (Analytical pure, KELON Chemical Reagent Factory, Chengdu, China). All of the GAC samples are dried for 2 days at 90 °C with the electric drying oven, except sample B, which was initially soaked in deionized water and then be frozen at −40 °C for 1 day. This process was done to physically enlarge the pore volume. The other samples were named as A, C1, C2 and C3. Generally, sample A was the blank, sample B was treated by freezing procedure, samples C1–C3 were treated by microwave irradiation with a modified domestic microwave oven. The modification involved replacing the magnetron by an industrial one, which is cooled by water and the model named as 2M410A. All of the samples C1–C3 were treated by a microwave in the same anode current 0.4 A, but for different durations (min). In addition, to prevent the GAC from over treatment and potentially burning down, the maximum microwave irradiation duration should be less than 3 min. Thus, in order to observe the effect of different microwave irradiation duration on the properties of GAC samples, the microwave irradiation duration for samples C1–C3 was set to be 1, 2, and 3 min, respectively.

3.2. Measurement and Characterization

(a) Measurement of the effective complex permittivity: resonant cavity method.

Specific measurement apparatus and particular principles were referenced in [17]. In general, the measurement system was composed of two parts:

- A metal can cavity and the accompanying open-end coaxial probe were well-designed. The can was finely manufactured with a fixed size. Thus, when the can was filled with the GAC samples, the heap volume V was the same as the volume of the can.
- A vector network analyzer (VNA) (N5230A, Agilent, Santa Rosa, United States) was used to measure the magnitude and phase of scattering parameter S11. Based on a well-trained back propagation (BP) neural network as the core algorithm, it was quite convenient to infer the effective complex permittivity of the sample.

(b) Measurement of the fundamental physical coefficient: the heap mass M, and the granule density ρ_g. A total of 20–30 grains of GAC were picked arbitrarily. The mass and geometric dimensions of each

granular was determined by electronic balance and vernier caliper, respectively. The data was used to calculate the arithmetic mean of the mass and volume for each grain. Finally, the mass of the granular was divided by the volume to obtain the density ρ_g.

(c) Characterization of the pore volume. Pore volume was determined using the automatic surface area

and pore analyzer (ASAP2020, Micromeritcs, Norcross, GA, USA). Nitrogen isotherm adsorption (at relative pressure of 0.99 atm) was used to calculate the pore volume by the static volumetric method.

4. Results and Discussion

The detailed experimental results are collected in Table 1.

Table 1. The detailed experimental data.

Marker	Treatment	ρ_g (g/cm^3)	M (g)	V (cm^3)	ε_{eff}	v_g (cm^3/g)
A	—	0.8214	424.757		6.419-j1.401	0.4219
B	Frozen	0.7072	431.935		5.824-j1.219	0.4801
C1		0.7791	404.441	785.398	4.233-j0.577	0.4718
C2	Microwave	0.7683	379.004		3.630-j0.544	0.5108
C3	Irradiation	0.7601	407.279		3.876-j0.629	0.4206
Average		0.7673	409.483		–	0.46104

In Table 1, compared the properties of sample A to sample B, it showed that the frozen process can enlarge the pore volume by about 13.8% or $(0.4801 - 0.4219)/0.4219$ and reduce the real and imaginary part of the complex permittivity by about 9.3% or $(6.419 - 5.824)/6.419$ and 13.0% or $(1.401 - 1.219)/1.401$, respectively. Similarly, the pore volume of samples C1–C3 was enlarged by the microwave irradiation, while the permittivity decreased accordingly. However, we can also noticed that when the microwave radiation duration reaches a certain extent, the pore volume of the sample will be decreased, as shown for sample C3 in Table 1. Therefore, in order to prevent the sample from over treatment and potentially burning down, a reasonable microwave radiation duration was required.

In order to further study the relationship between the pore volume and the permittivity of the GAC samples, we take the average density ($\overline{\rho_g}$ = 0.7673 g/cm^3) and heap mass ($\overline{M}$ = 409.483 g) to represent the GAC's granule density and heap mass, respectively. Substituting $\overline{\rho_g}$, $\overline{M}$, the heap volume (V = 785.398 cm^3) and the measured pore volume (v_g) of each GAC in Table 1 into Equations (5), (8), and (11), we can obtain the ε_{GAC}^t in both Model A and Model B. The results are presented in Tables 2 and 3.

Table 2. The complex permittivity of the ideal perfect granular activated carbon (GAC) in Model A.

Marker	Treatment	ε_{GAC}^t	$\tan\delta\left(\varepsilon_{GAC}^t\right)$
A	—	17.750-j4.460	0.2513
B	Frozen	12.789-j3.071	0.2402
C1		11.169-j1.896	0.1697
C2	Microwave Irradiation	10.191-j2.000	0.1963
C3		8.883-j1.804	0.2031

Table 3. The complex permittivity of the ideal perfect GAC in Model B.

Marker	Treatment	ε_{GAC}^t	$\tan\delta\left(\varepsilon_{GAC}^t\right)$
A	—	16.875-j4.180	0.2477
B	Frozen	12.411-j2.945	0.2373
C1		10.683-j1.776	0.1663
C2	Microwave Irradiation	9.708-j1.858	0.1914
C3		8.590-j1.711	0.1992

From Tables 2 and 3, we can clearly see that the results obtained by Model A are slightly better than those obtained by Model B. The maximum difference of the real and imaginary part of complex permittivity and the loss tangent $\tan\delta\left(\varepsilon_{GAC}^t\right)$ obtained by model A and model B is 4.930%

or $(17.750 - 16.875)/17.750$, 7.100% or $(2.000 - 1.856)/2.000$, and 2.496% or $(0.1963 - 0.1914)/0.1963$, respectively. Nevertheless, under the condition that there are individual differences in the samples, Tables 2 and 3 verified that model A and B could provide the results with little difference. Hence, in the following discussion, we just take the data of Model A into account. Considering that the loss tangent plays a crucial role in microwave heating, the results can be clearly grouped according to whether it was processed with microwave. To illustrate this more specifically, we take the average of the non-microwave treatment samples A and B:

$$\varepsilon_{GAC}^{t} = \overline{\varepsilon_{GAC}^{t}} = 15.269 - j3.766 \tag{12}$$

Substituting $\overline{\rho_g}$, $\overline{M}$, V, and Equations (12) into (8), we can derive the relationship between ε_{eff} and v_g, as shown in Figure 2. Similarly, the relationship between $\tan \delta(\varepsilon_{eff})$ and v_g can also be obtained, as shown in Figure 3.
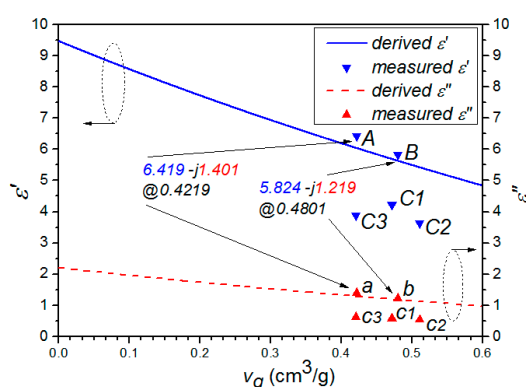

Figure 2. Theoretical and experimental comparison graph between ε_{eff} (ε'-jε'') and v_g.
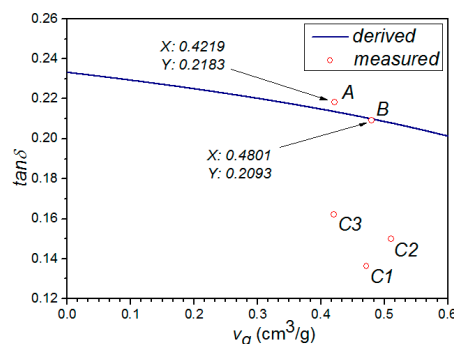

Figure 3. Theoretical and experimental comparison graph between $\tan \delta(\varepsilon_{eff})$ and v_g.

In Figures 2 and 3, it can be clearly seen that the properties of samples A and B fit the derived curve well, while those of samples C1–C3 have a considerable shift from the curve. It indicated that microwave treatment have a significant effect on the structure of GAC, making the classical model no longer suitable for describing its permittivity. This is reasonable, because the derivation in both Model A and Model B did not take the microwave factor into account. Meanwhile, we can also notice that both ε_{eff} and $\tan \delta(\varepsilon_{eff})$ are decreased with the increment of v_g. This may be due to the fact that the air (low permittivity) composition in mixture increases with the increment of v_g.

5. Conclusions

This paper studied the relationship between the effective complex permittivity and pore volume of GAC. The relationship was derived based on MGA theory. Two quantificational expressions were

established in different equivalent models, respectively. A well-designed resonant cavity and the accompanying open-end coaxial probe were introduced to measure the effective complex permittivity of the GAC. The automatic surface area and pore analyzer was also applied to carry out the BET testing to acquire the pore volume of the GAC. Results obtained by the two expressions were extremely similar. Meanwhile, the theoretical results are in a good agreement with those from the experiment. In addition, the results indicated that microwave treatment had a great impact on the structure of GAC, making the classical model no longer suitable for describing its permittivity.

This study provided a bridge to link the effective complex permittivity and pore volume of GAC. In addition, it provided a potential and convenient method for the rapid assisted characterization of GAC. In the future study, we will try to take the microwave factor into account during derivation, and study the relationship between the permittivity and pore size distribution or different absorbability (porosity).

Author Contributions: Yang Yang conceived and designed the experiments; Chao Shi and Yi Zhang performed the experiments; Yang Yang developed the model, analyzed the data and wrote the initial draft of the manuscript; Jinghua Ye reviewed and contributed to the final manuscript; Huangcheng Zhu and Kama Huang contributed the location and equipment.

Conflicts of Interest: The authors declare no conflict of interest.

References

1. Mohan, D.; Singh, K.P. Granular Activated Carbon. In *Water Encyclopedia*, 1st ed.; John Wiley & Sons, Inc.: Hoboken, NJ, USA, 2005; pp. 92–107.

2. Walker, G.M.; Weatherley, L.R. Adsorption of acid dyes on to granular activated carbon in fixed beds. *Water Res.* **1997**, *31*, 2093–2101. [CrossRef]

3. Yin, C.Y.; Aroua, M.K.; Wan, M.A. Review of modifications of activated carbon for enhancing contaminant uptakes from aqueous solutions. *Sep. Purif. Technol.* **2007**, *52*, 403–415. [CrossRef]

4. Dias, J.M.; Alvim-Ferraz, M.C.M.; Almeida, M.F.; Rivera-Utrilla, J.; Sánchez-Polo, M. Waste materials for activated carbon preparation and its use in aqueous-phase treatment: A review. *J. Environ. Manag.* **2007**, *85*, 833–846. [CrossRef] [PubMed]

5. Karmakar, M.K.; Chandra, P.; Chatterjee, P.K. A review on the fuel gas cleaning technologies in gasification process. *J. Environ. Chem. Eng.* **2015**, *3*, 689–702.

6. Liu, X.; Quan, X.; Bo, L.; Chen, S.; Zhao, Y. Simultaneous pentachlorophenol decomposition and granular activated carbon regeneration assisted by microwave irradiation. *Carbon* **2004**, *42*, 415–422. [CrossRef]

7. Liu, X.; Yu, G.; Han, W. Granular activated carbon adsorption and microwave regeneration for the treatment of 2,4,5-trichlorobiphenyl in simulated soil-washing solution. *J. Hazard. Mater.* **2007**, *147*, 746–751. [CrossRef] [PubMed]

8. Liu, Q.S.; Wang, P.; Zhao, S.S.; Zhang, W. Treatment of an industrial chemical waste-water using a granular activated carbon adsorption-microwave regeneration process. *J. Chem. Technol. Biotechnol.* **2012**, *87*, 1004–1009. [CrossRef]

9. Ania, C.O.; Parra, J.B.; Menéndez, J.A.; Pis, J.J. Effect of microwave and conventional regeneration on the microporous and mesoporous network and on the adsorptive capacity of activated carbons. *Microporous Mesoporous Mater.* **2005**, *85*, 7–15. [CrossRef]

10. Shi, C.; Wang, T.; Zhang, F.H.; Hua, J.; Huang, K.M.; Yang, Y. Study on regeneration of granular activated carbon by microwave thermal treatment. *J. Sichuan Univ. Sci. Ed.* **2015**, *52*, 101–106.

11. Pelekani, C.; Snoeyink, V.L. Competitive adsorption between atrazine and methylene blue on activated carbon: The importance of pore size distribution. *Carbon* **2000**, *38*, 1423–1436. [CrossRef]

12. Li, L.; Quinlivan, P.A.; Knappe, D.R.U. Effects of activated carbon surface chemistry and pore structure on the adsorption of organic contaminants from aqueous solution. *Carbon* **2002**, *40*, 2085–2100. [CrossRef]

13. Lu, Q.; Sorial, G.A. The role of adsorbent pore size distribution in multicomponent adsorption on activated carbon. *Carbon* **2004**, *42*, 3133–3142. [CrossRef]

14. Lu, Q.; Sorial, G.A. Adsorption of phenolics on activated carbon—Impact of pore size and molecular oxygen. *Chemosphere* **2004**, *55*, 671–679. [CrossRef] [PubMed]

15. Chen, Q.; Yang, Y.; Huang, K.M.; Chen, C.; Wang, K.Y. A permittivity measurement method based on cavity perturbation technique. *Appl. Mech. Mater.* **2014**, *590*, 629–633. [CrossRef]

16. Chen, F.; Mao, S.; Wang, X.; Semouchkina, E.; Lanagan, M. Effects of cavity dimensions in split-post dielectric resonator technique for complex permittivity measurements. In Proceedings of the 2012 IEEE Antennas and Propagation Society International Symposium (APSURSI), Chicago, IL, USA, 8–14 July 2012; pp. 1–2.

17. Chen, Q.; Huang, K.M.; Yang, X.; Luo, M.; Zhu, H. An artificial nerve network realization in the measurement of material permittivity. *Prog. Electromagn. Res.* **2011**, *116*, 347–361. [CrossRef]

18. Eichelbaum, M.; Stößer, R.; Karpov, A.; Dobner, C.K.; Rosowski, F.; Trunschke, A.; Schlögl, R. The microwave cavity perturbation technique for contact-free and in situ electrical conductivity measurements in catalysis and materials science. *Phys. Chem. Chem. Phys.* **2012**, *14*, 1302–1312. [CrossRef] [PubMed]

19. Chen, L.; Ong, C.K.; Tan, B.T.G. Amendment of cavity perturbation method for permittivity measurement of extremely low-loss dielectrics. *IEEE Trans. Instrum. Meas.* **1999**, *48*, 1031–1037. [CrossRef]

20. Roelvink, J.; Trabelsi, S. Measuring the complex permittivity of poultry meat with a planar transmission-line sensor. In Proceedings of the 2013 IEEE International Instrumentation and Measurement Technology Conference, Minneapolis, MN, USA, 6–9 May 2013; pp. 1689–1693.

21. Adous, M.; Quéffélec, P.; Laguerre, L. Coaxial/cylindrical transition line for broadband permittivity measurement of civil engineering materials. *Meas. Sci. Technol.* **2006**, *17*, 2241. [CrossRef]

22. Baker-Jarvis, J.; Vanzura, E.J.; Kissick, W.A. Improved technique for determining complex permittivity with the transmission/reflection method. *IEEE Trans. Microw. Theory Tech.* **1990**, *38*, 1096–1103. [CrossRef]

23. Garnett, J.M. Colours in metal glasses and in metallic films. *Philos. Trans. R. Soc. Lond.* **1904**, *73*, 443–445. [CrossRef]

24. Mallet, P.; Guerin, C.A.; Sentenac, A. Maxwell-Garnett mixing rule in the presence of multiple scattering: Derivation and accuracy. *Phys. Rev. B* **2005**, *72*, 014205. [CrossRef]

25. Li, S.; Chen, R.; Anwar, S.; Lu, W.; Lai, Y.; Chen, H.; Hou, B.; Ren, F.; Gu, B. Applying effective medium theory in characterizing dielectric constant of solids. *Prog. Electromagn. Res. Lett.* **2012**, *35*, 145–153. [CrossRef]